不純物流入モニター(ダイバータ)の開発
及び
イーターに向けた
原子分子素過程の必要性

岩前敦, 杉江達夫, 小川宏明, 河西敏[†] , 草間義紀
JAEA, [†]NAT

ITER

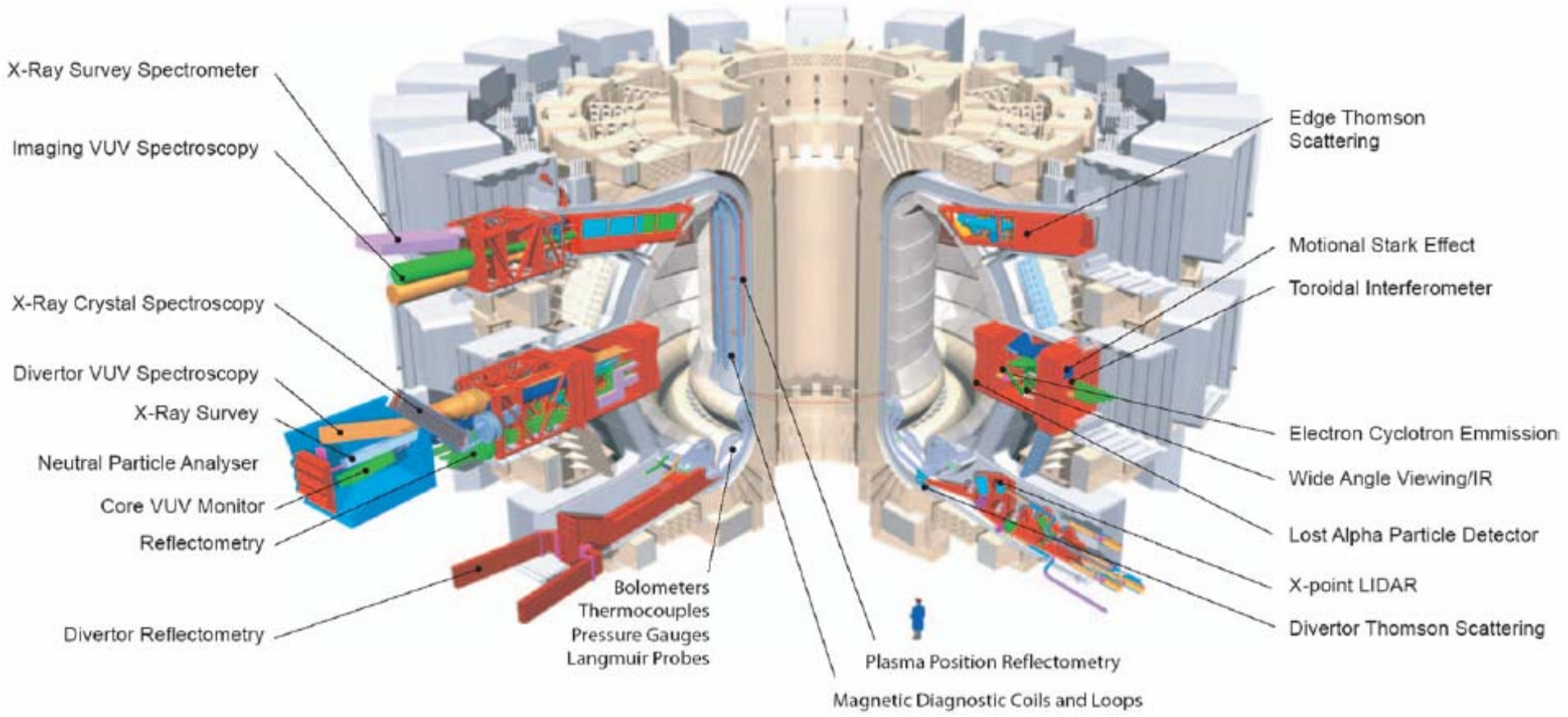

Figure 15. Cut-out view of ITER to visualize some typical diagnostics in upper and equatorial ports, as well as in the diagnostic divertor cassettes.

Composition of ITER plasma

fusion reaction : D, T, He

material on PFC: Be, C, W

impurity seeding

for core control: Ne, Ar, Kr

Plasma conditions

Core: T ~ 0.2 - 20 keV, n~10^{20} m^{-3}

Edge: neutrals,

T~0.1-200 eV, n~10^{18} – 10^{21} m^{-3}

Specification for plasma measurements on ITER - impurity influx monitor (divertor) -

Measurement	Parameter	Condition	Range or Coverage	Resolution: Time or Freq.	Resolution: Spatial or Wave No.	Accuracy
12. Impurity species monitoring	Be, C rel. conc.		10^{-4}–5×10^{-2}	10 ms	Integral	10% (rel.)
	Be, C influx		4×10^{16}–2×10^{19} s^{-1}	10 ms	Integral	10% (rel.)
	Cu rel. conc.		10^{-5}–5×10^{-3}	10 ms	Integral	10% (rel.)
	Cu influx		4×10^{15}–2×10^{18} s^{-1}	10 ms	Integral	10% (rel.)
	W rel. conc.		10^{-6}–5×10^{-4}	10 ms	Integral	10% (rel.)
	W influx		4×10^{14}–2×10^{17} s^{-1}	10 ms	Integral	10% (rel.)
	Extrinsic (Ne,Ar, Kr) rel. Conc.		10^{-4}–2×10^{-2}	10 ms	Integral	10% (rel.)
	Extrinsic (Ne, Ar, Kr)		4×10^{16}–8×10^{18} s^{-1}	10 ms	Integral	10% (rel.)
35. Impurity and D,T influx in the divertor	Γ_{Be}, Γ_C, Γ_W		10^{17}–10^{22} at s^{-1}	1 ms	50 mm	30%
	Γ_D, Γ_T		10^{19}–10^{25} at s^{-1}	1 ms	50 mm	30%
39. Divertor helium density	n_{He}		10^{17}–10^{21} m^{-3}	1 ms	—	20%
40. Fuel ratio in the divertor	n_T/n_D		0.1–10	100 ms	integral	20%
	n_H/n_D		0.01–0.1	100 ms	integral	20%

Progress in the ITER Physics Basis

A.J.H Donné, A.E. Costley, R. Barnsley et al. Nuclear Fusion 47 (2007) S337-S384

Upper Port Plug

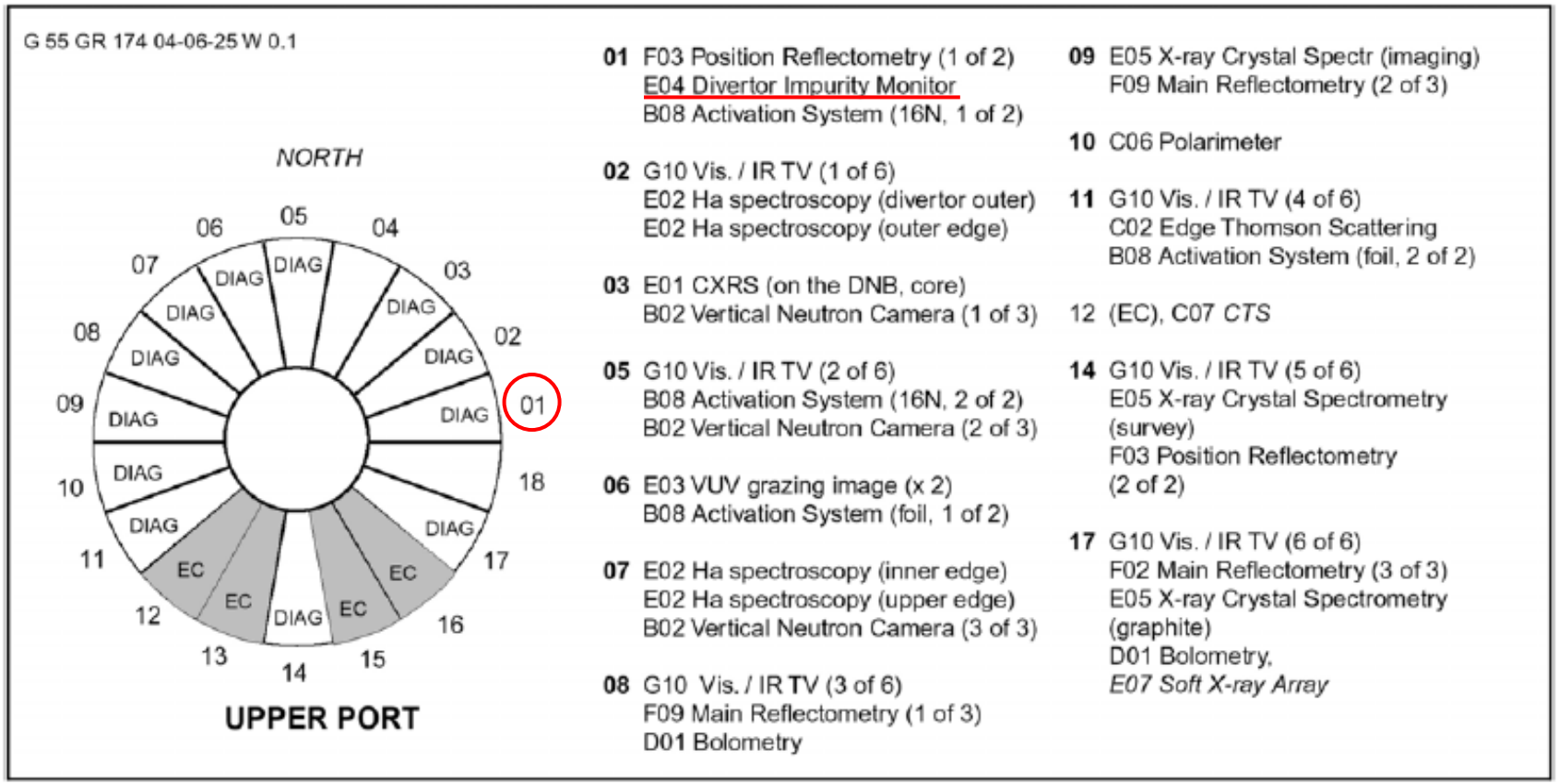

Figure 20. Allocation of upper port plug diagnostics.

Equatorial Port Plug

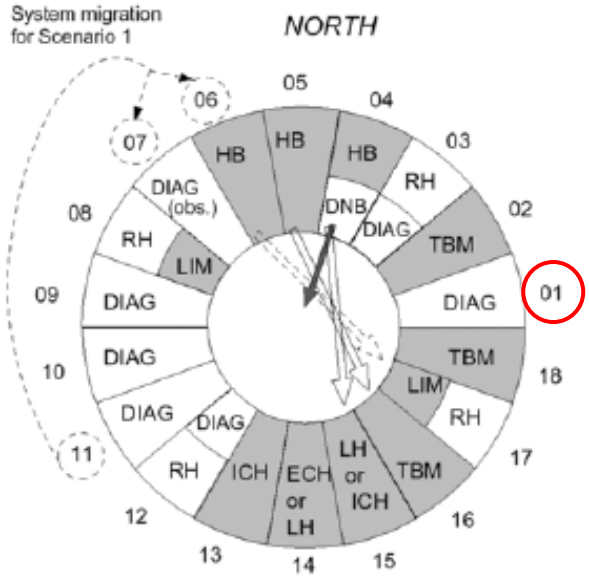

EQUATORIAL PORT

01 G01 Vis. / IR TV (1 of 4)
B01 Radial Neutron Camera
D01 Bolometry,
E11 MSE (core, HB4)
E04 Divertor Impurity Monitor
B07 Gamma Ray Spectroscopy
B11 High Resolution Neutron Spectr

03 G01 Vis. / IR TV (2 of 4)
E12 CXRS (on the DNB)
E11 MSE (edge, HB5)
E02 Ha Spectroscopy (divertor inner)

07 B08 Activation System (16N, 1 of 2)
B08 Activation System (foil, 1 of 2)
B04 Neutron Flux Monitor (DD)

08 B04 Neutron Flux Monitor (DT)

09 G01 Vis. / IR TV (3 of 4)
C05 Toroidal Interferometer/Polarimeter
E05 X-Ray Crystal Spect (Imaging)
F01 ECE,
F07 Fast Wave Reflectometry
E07 Soft X-ray Array

10 C01 Thomson Scattering main plasma)
C06 Polarimeter
C08Thomson Scattering (inner divertor)

11 E05 X-ray Crystal Spect (survey)
E03 VUV (main and divertor)
F02 Reflectometry (main plasma)
E08 NPA

12 G01 Vis. / IR TV (4 of 4)
E02 Ha Spect (upper edge)
E06 Visible Continuum Array
C07 CTS

17 B04 Neutron Flux Monitor (DT)
B08 Activation System (16N, 1 of 2)
B08 Activation System (foil, 2 of 2)

Figure 18. Allocation of diagnostics to equatorial ports (showing relocation of systems on port 11 which will be necessary if heating upgrade scenario 1 (additional RF systems) is selected).

Divertor Port Plug

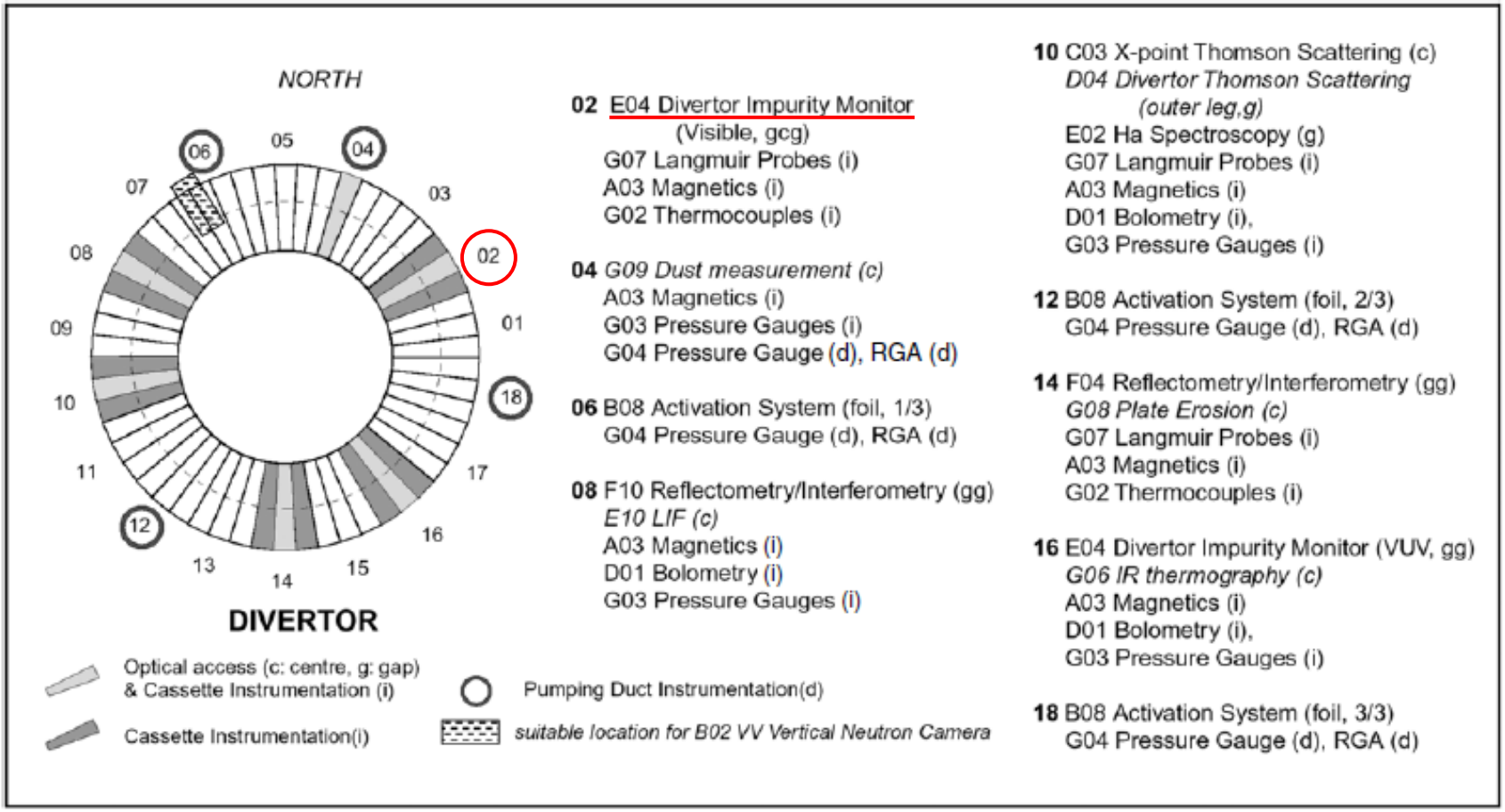

Figure 22. Allocation of diagnostics and other systems at the divertor.

Arrangement of the lines of sight

●Main functions : to identify **impurity species** and to measure **two-dimensional distributions of particle influx densities** in the divertor plasmas by means of spectroscopic techniques in the wavelength range of 200 - 1000 nm.

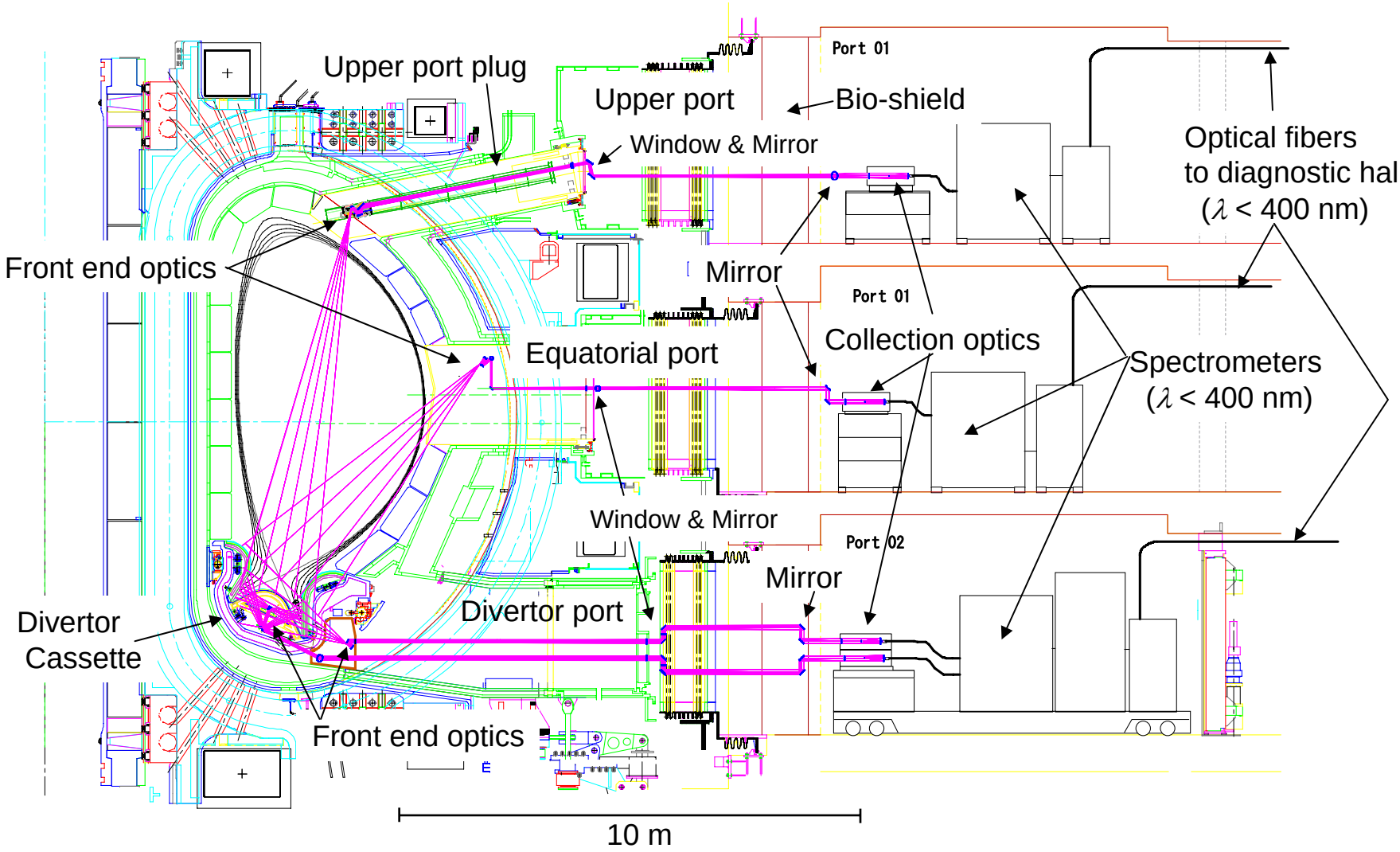

Overview of Spectrometer

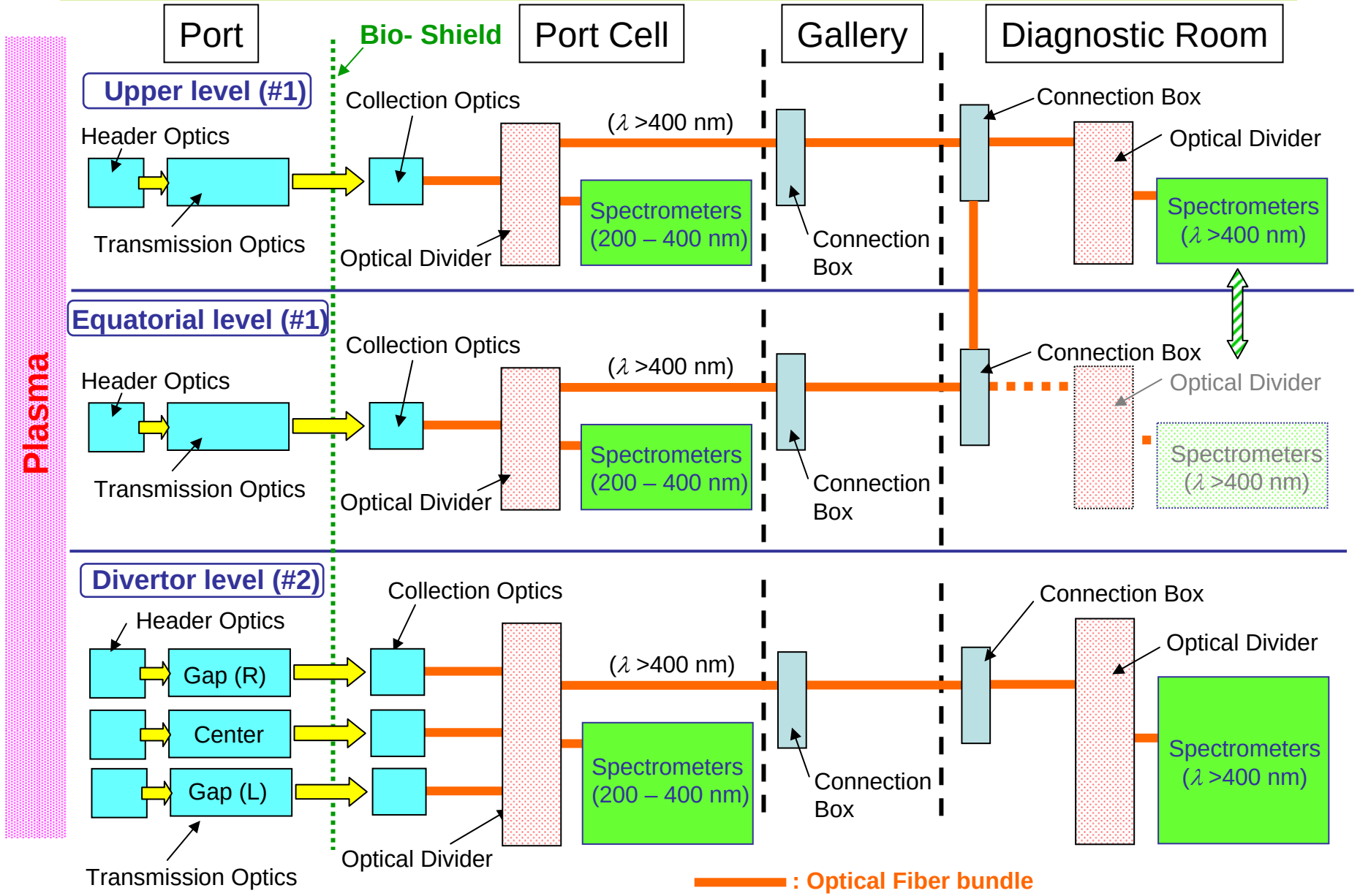

Impurity Influx Monitor (divertor)

- The divertor impurity monitor composed of three different types of spectrometers has been designed.

• Visible survey spectrometer

Parameters to be measured:	Impurity species, Impurity and D/T influx
Wavelength range:	200 nm - 1000 nm (simultaneously)
Wavelength resolution:	~ 0.1 nm
Time resolution:	>10 ms
Spatial resolution:	~ 10 mm

• Filter spectrometer

Parameters to be measured:	2-dimensional impurity and D/T influx, Ionization front,
Wavelength range:	200 nm - 1000 nm (~ 12 spectral lines simultaneously)
Wavelength resolution:	~ 1 nm
Time resolution:	~ 1 ms
Spatial resolution:	~ 10 mm

• High dispersion spectrometer

Parameters to be measured:	n_T/n_D and n_H/n_D ratio, Ion temperature (velocity)
Wavelength range:	200 nm - 1000 nm
Wavelength resolution:	< 0.01 nm
Time resolution:	>10 ms
Spatial resolution:	~ 10 mm

Optical Design of Upper Port and Port Integration

- From calculation by ZEMAX code, the spatial resolution of 37 mm will be achieved for all lines of sight.
- Integration these optical components to the Up #1port is performed.
- As a result of the integration in the upper port, optical components of the front-end optics were installed inside the pipe with inner diameter of 300 mm replaced with that for the remote-handling of the port plug.

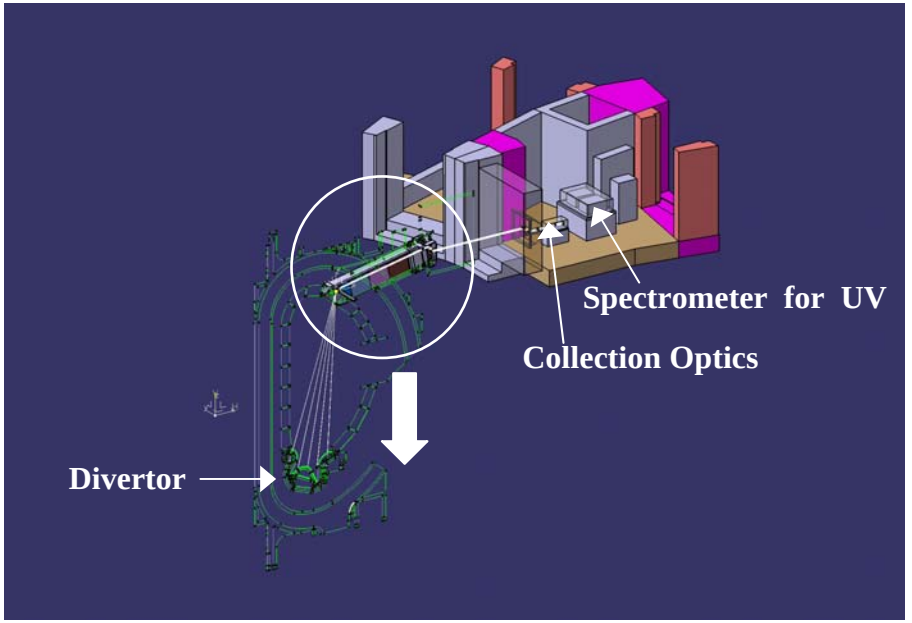

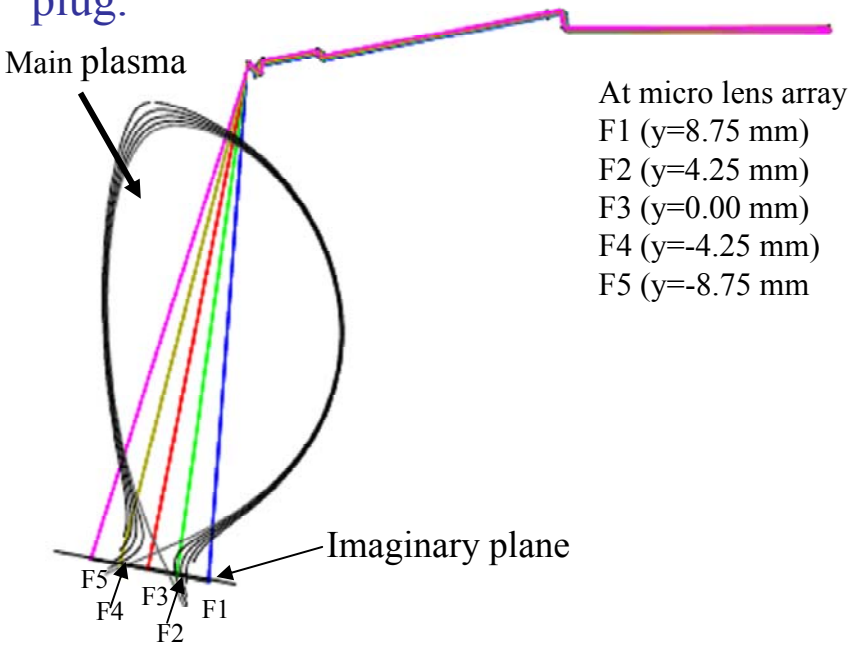

At micro lens array
F1 (y=8.75 mm)
F2 (y=4.25 mm)
F3 (y=0.00 mm)
F4 (y=-4.25 mm)
F5 (y=-8.75 mm

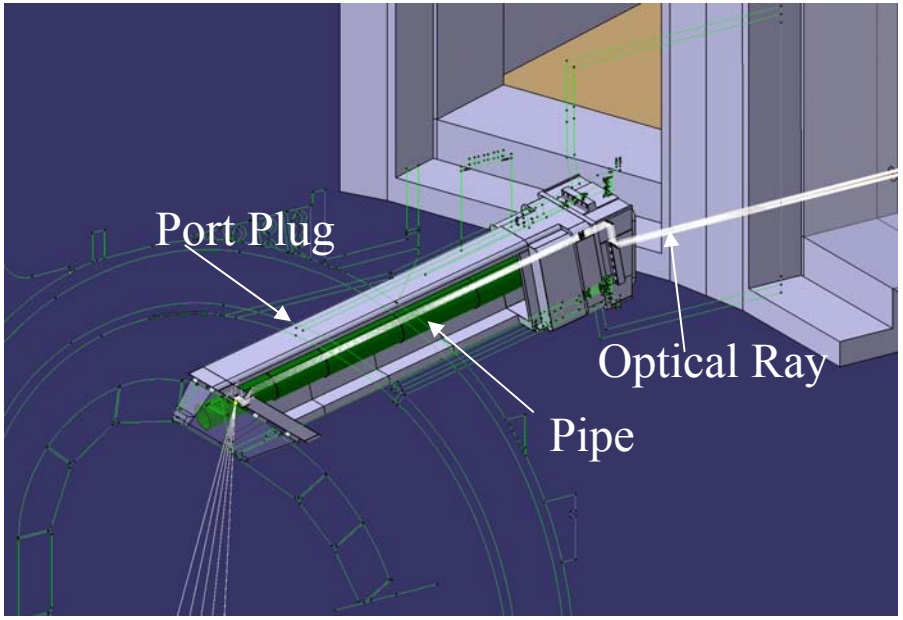

Mechanical Design of Front End Optics of Upper Port

- Three mirrors can be installed on the mirror mounting module with 300 mm diameter. It is also used for a neutron shielding and cooling the mirror.
- The kinematic mounting is used to adjust tilt angel of the first mirror before the installation on the port.
- The cupper mesh is connected from the first mirror to mirror mounting module to enhance the thermal conduction.

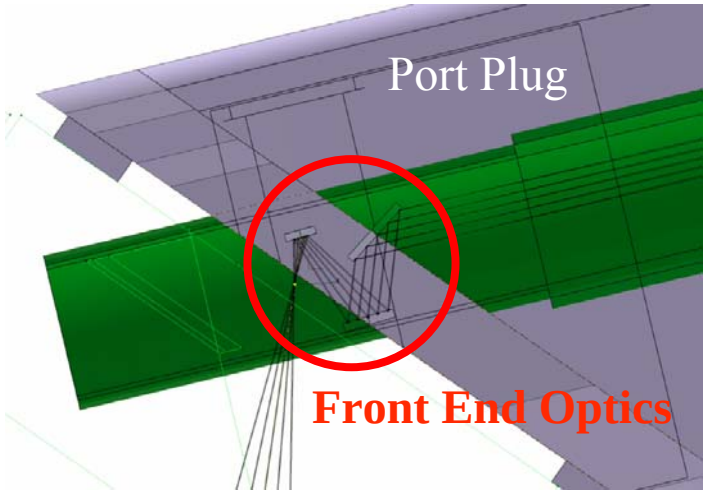

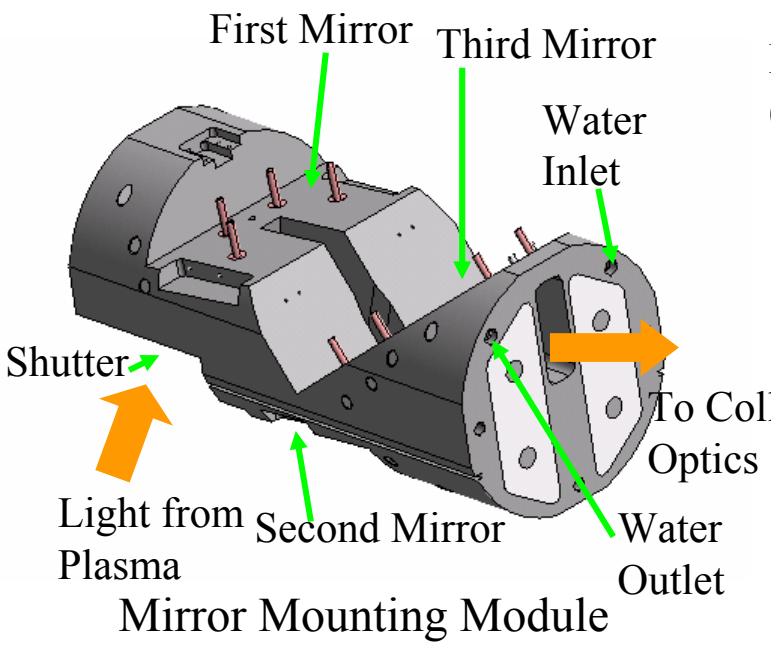

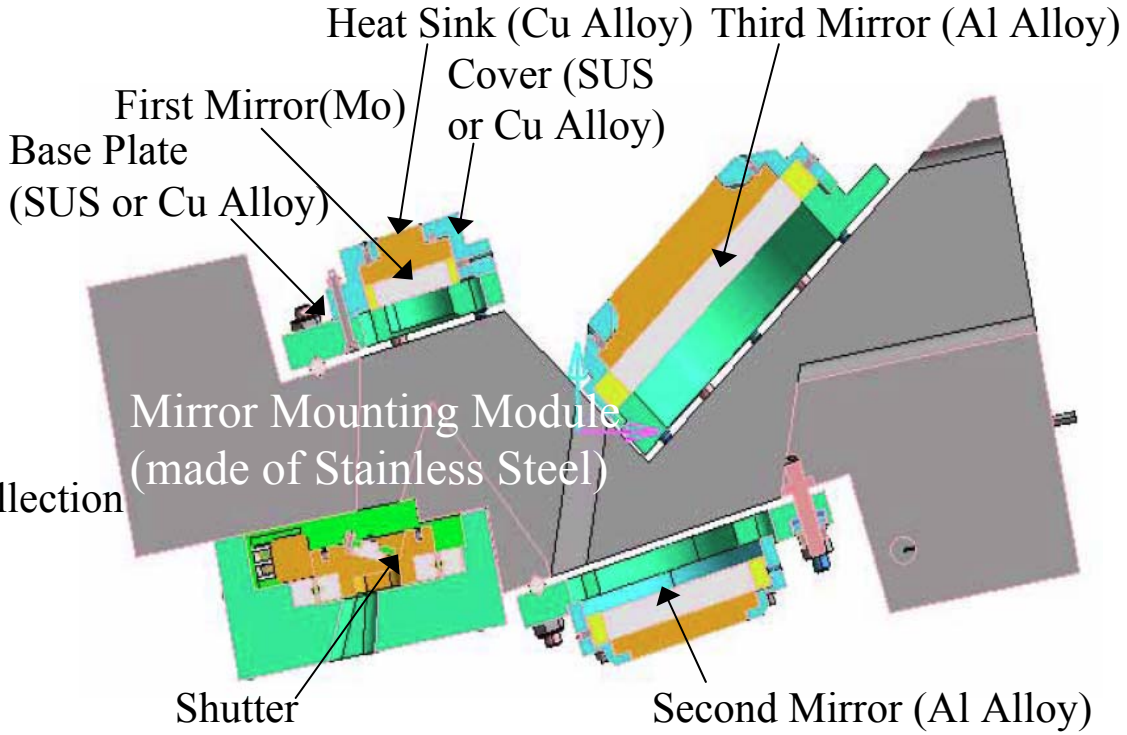

Mechanical Design of Shutter

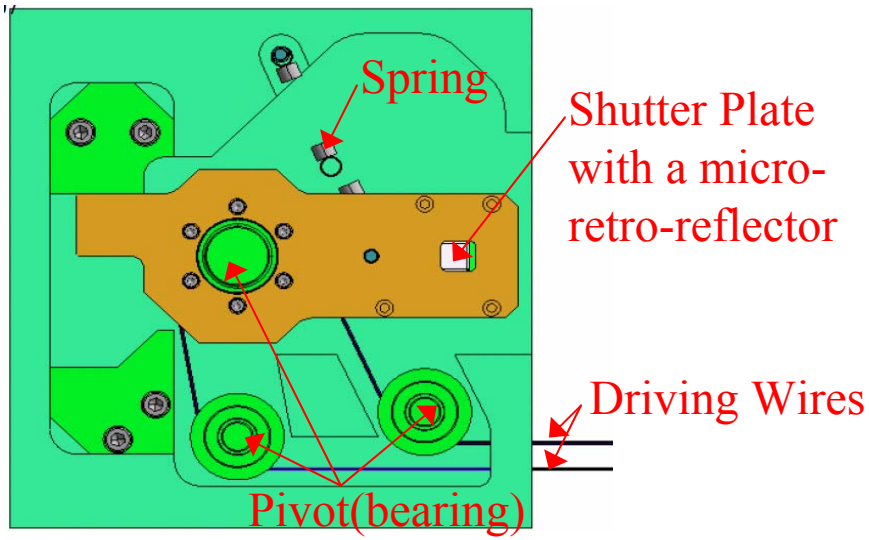

Rotary Motion Shutter driven by the Wire

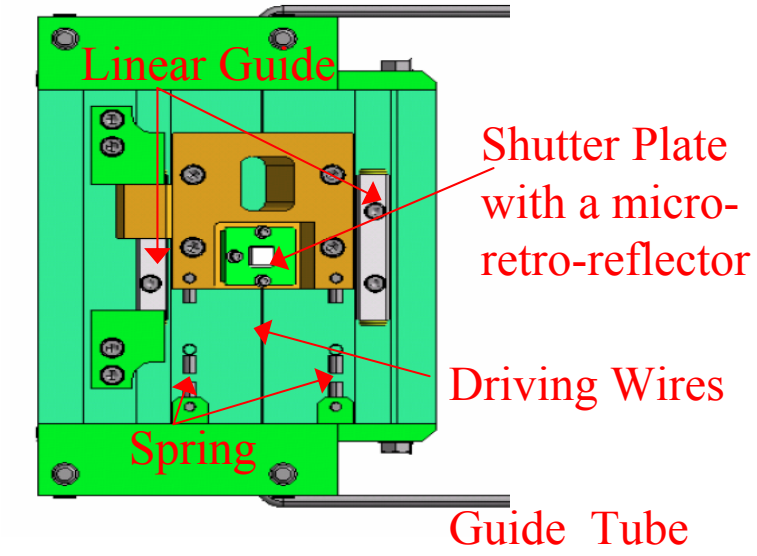

Linear Motion Shutter driven by the Wire

- Three type of shutter are designed.
- The shutter plate has a micro-retoro-reflector for the in-situ calibration.
- This shutter is mainly used during the discharge cleaning.
- Bearing and linear guide made of ceramic are used in this design.
- To compensate the thermal expansion of wire, the wire tension adjuster is also designed.

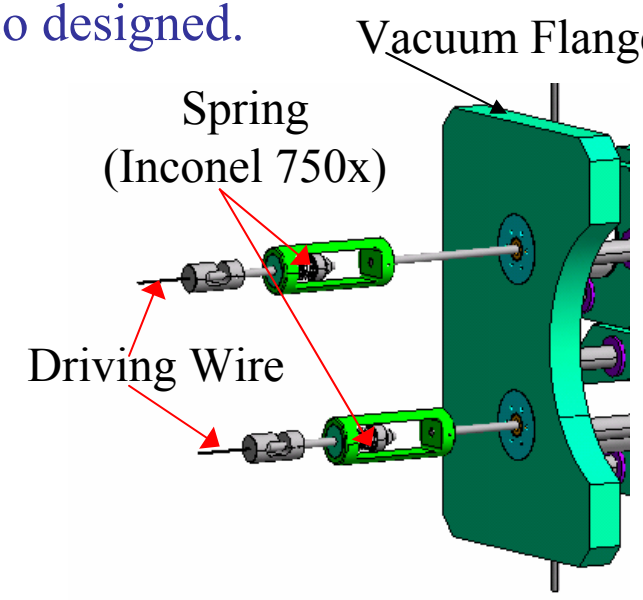

Wire Tension Adjuster

Steady-State Heat Analysis

- Only nuclear heating is considered in this analysis.
- Temperature rise of the mirror and mirror mounting module is less than 60 °C.
- Temperature profile is almost symmetric against the optical path.
- The maximum thermal strain is about 0.15 mm calculated assuming that position of 3 point of mirror mounting module is fixed.

Cooling Channel

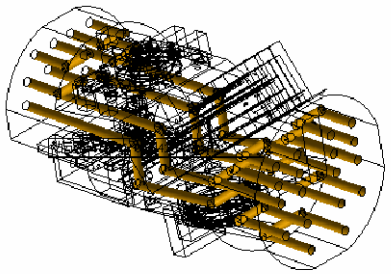

Flow Rate of Cooling Water : 5 (l/min)
Nuclear Heating : 2 x 10^{-4} (W/mm^3)
Cooling Water Temperature : 150 (℃)
Thermal Conductivity : 686.4 (mW/m・K)
Heat Transfer Rate : 4.29 x 10^{-3} (W/mm^2/K)
Initial Temperature : 150℃

Temperature Profile

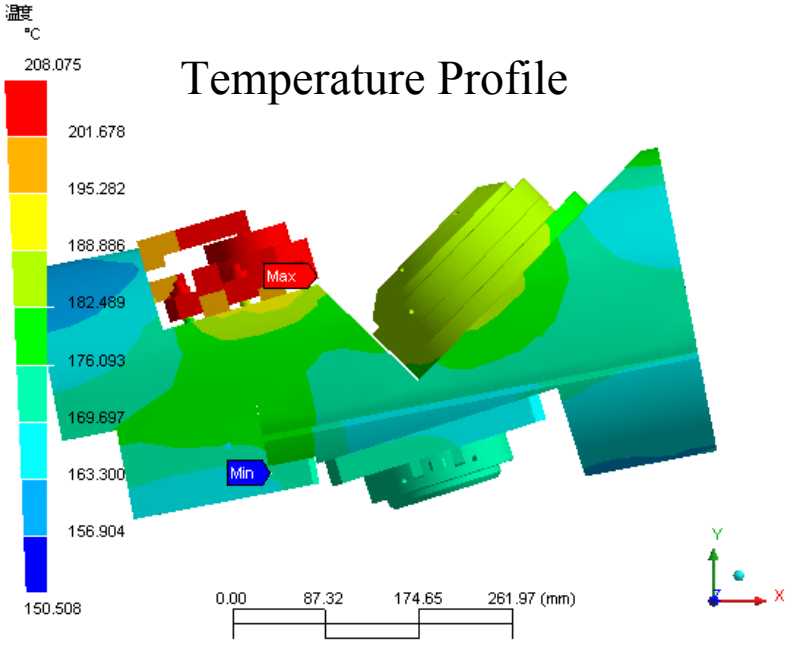

Thermal Strain Profile

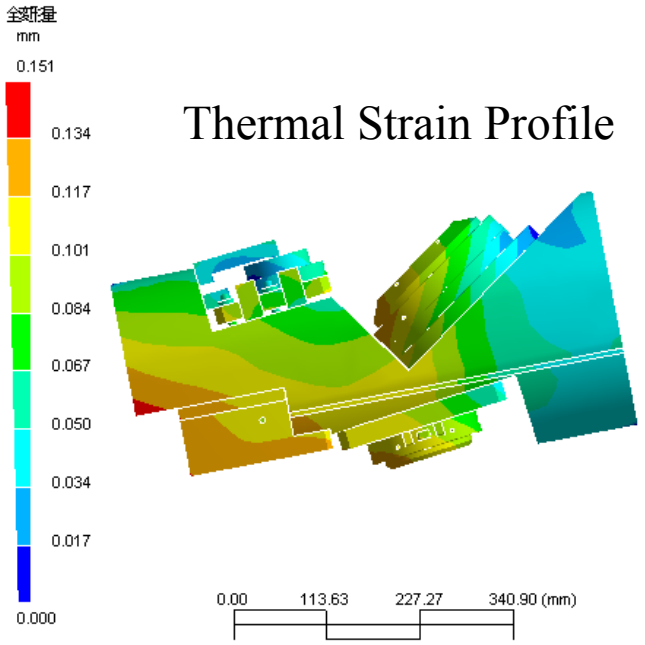

Fixed Point

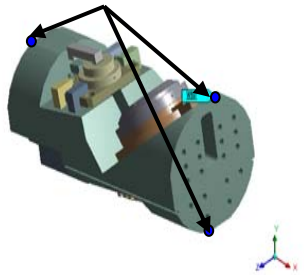

Optical Design of Divertor Port and Port Integration for previous divertor cassette

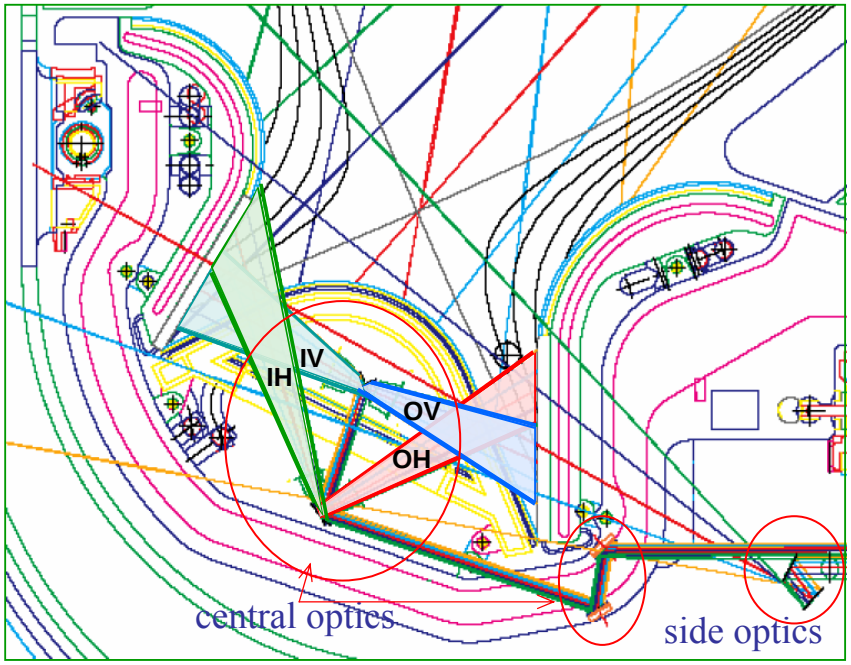

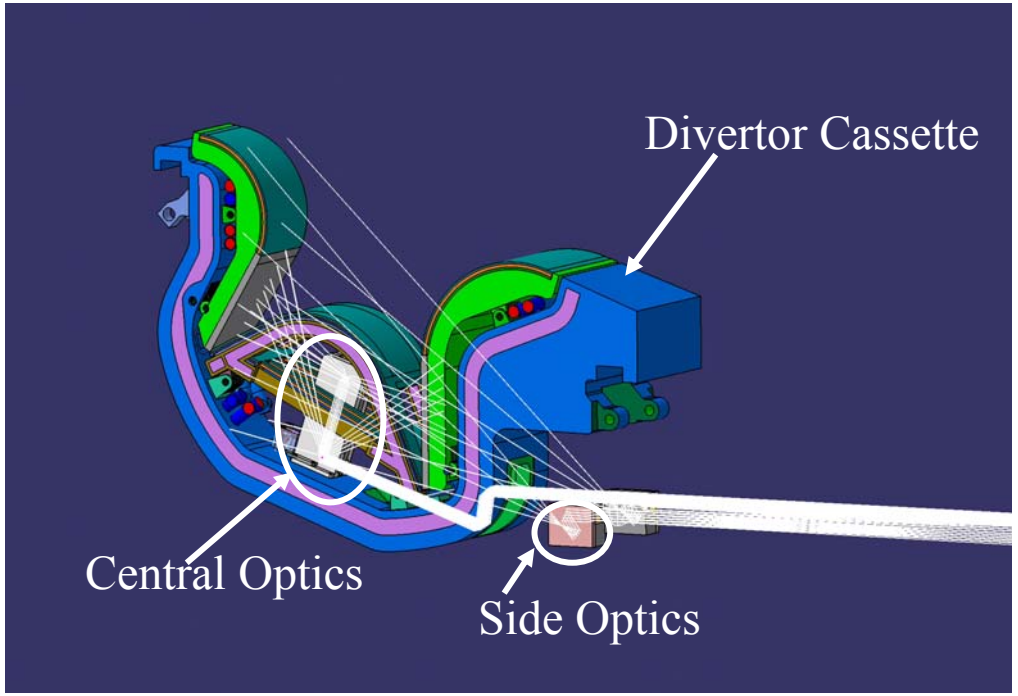

Computerized Tomography at the divertor

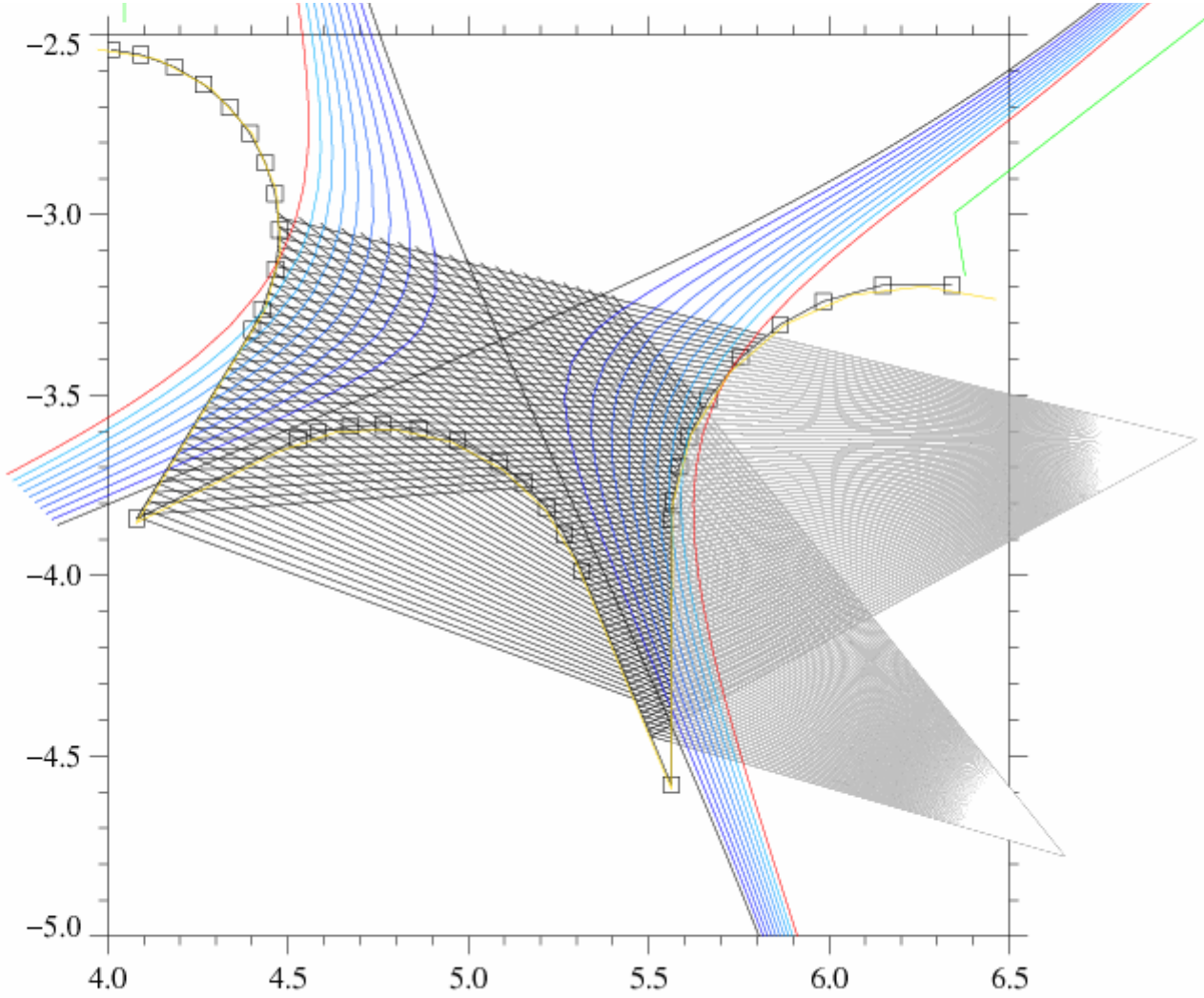

Computerized Tomography at the divertor

Model distribution

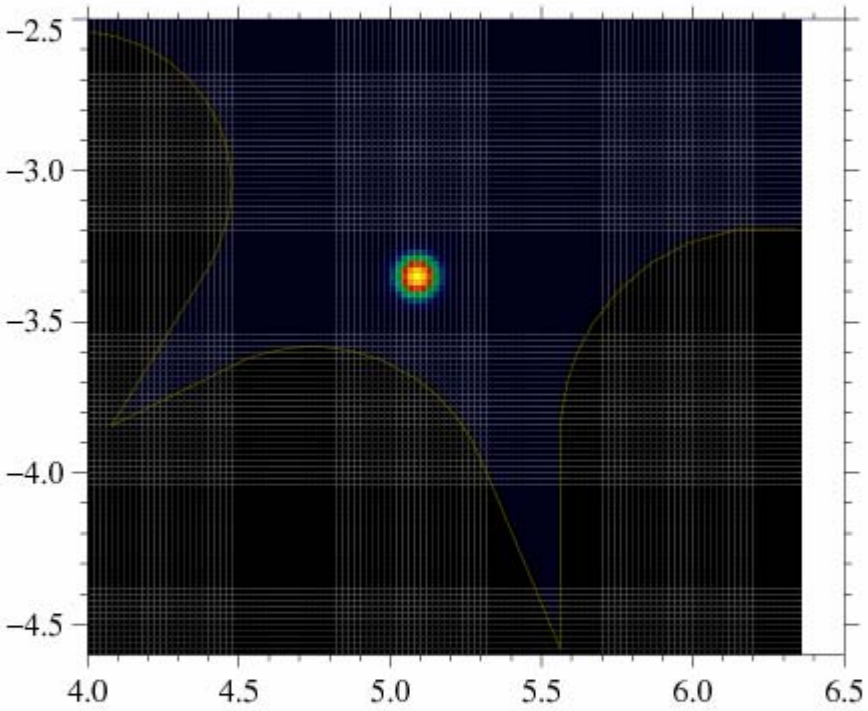

CT reconstructed image

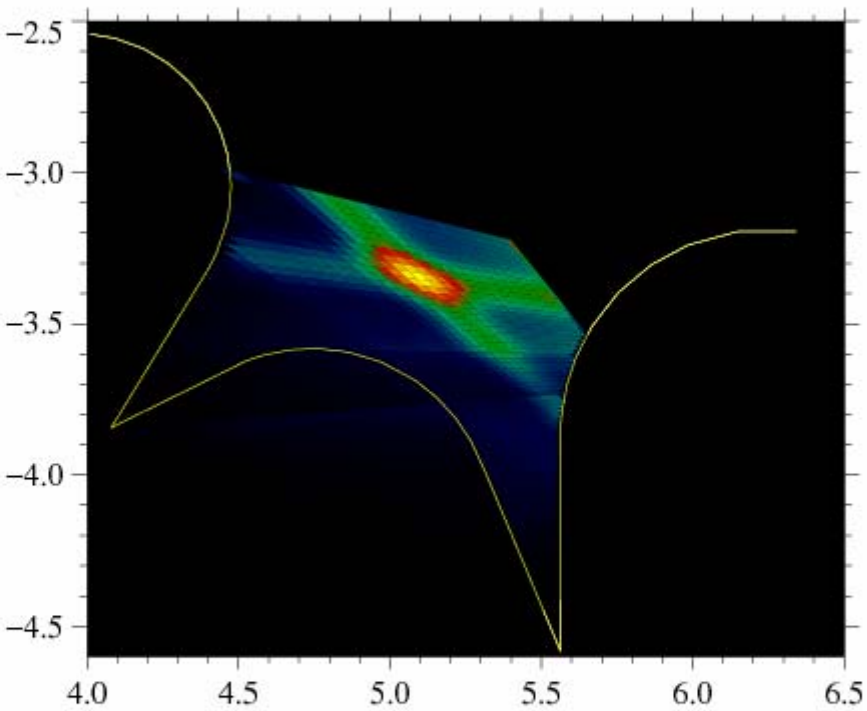

CT Code: Dr. K. Fujimoto (JT-60U G)

material of the plasma facing components

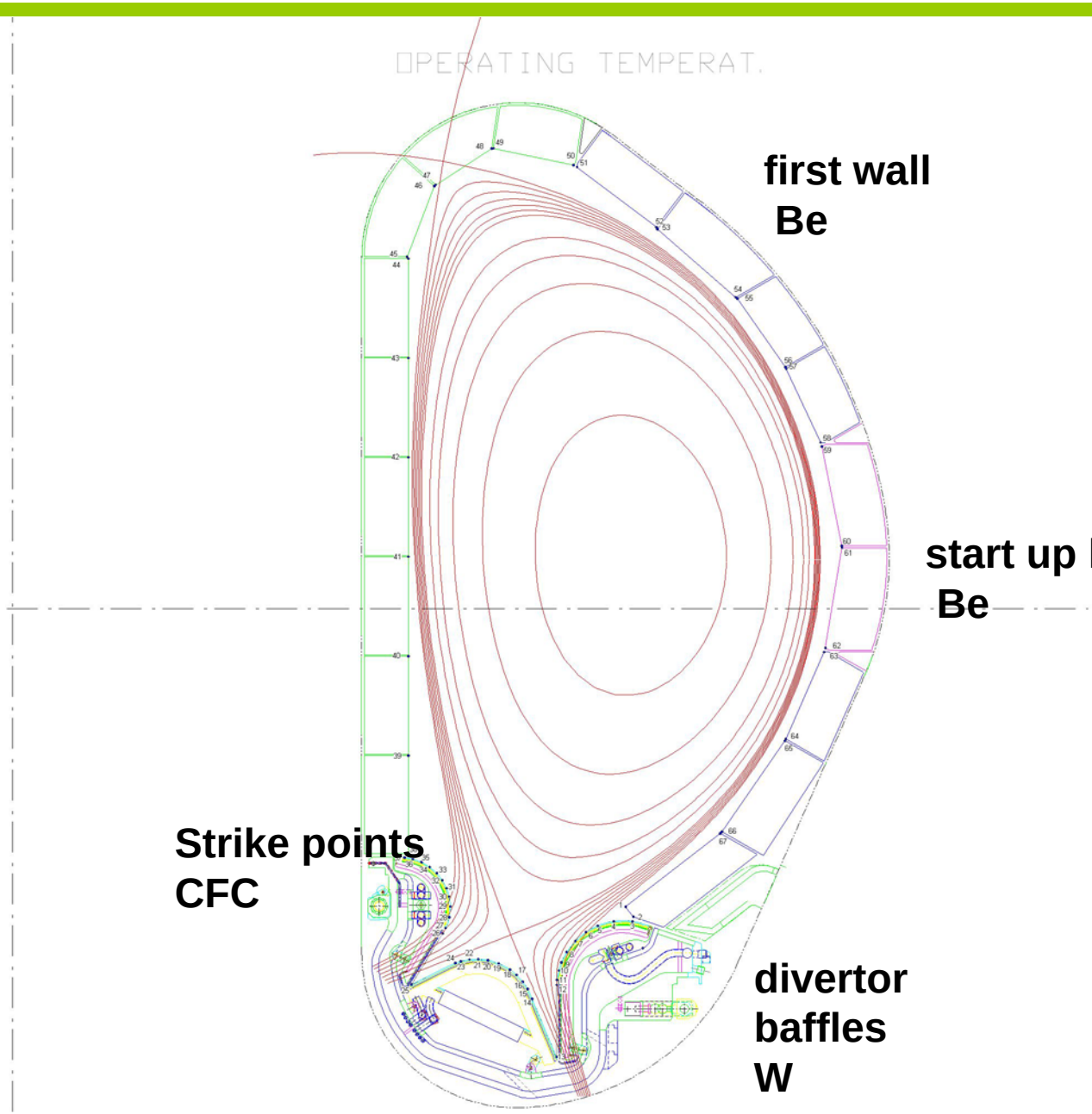

first wall
Be

start up limiter
Be

Strike points
CFC

divertor
baffles
W

ITER-like wall Project (JET)

EFDA JET

a member of EIROforum

About JET | EFDA | FUSION BASICS | FOCUS ON | JET & ITER | MULTIMEDIA | PUBLICATIONS | CONFERENCES

News : Site Map : FAQ : Contact : Links Search

Home > JET & ITER >

JET and ITER

- About ITER
- JET's capabilities in support of ITER
- **ITER-like Wall Project**
- Neutral Beam Enhancement Project
- High Frequency Pellet Injector Project
- Diagnostics and Plasma Control

ITER-like Wall Project

One of the main challenges for fusion reactors is the compatibility between a reactor-grade plasma and the materials facing the plasma (the "First Wall"). Most current tokamaks (including JET) use carbon composite (CFC) tiles for the First Wall, as does the Space Shuttle, which use it on the wings to withstand extreme heat fluxes. However, from JET's D-T experiments it is obvious that carbon composites are not suitable for the tritium operation due to high carbon migration, leading to tritium deposition in walls. Therefore the ITER design comprises a beryllium-clad First Wall in the main chamber, while use of carbon tiles is limited to the region where the edge plasma is deflected on to the wall ("divertor strike points") and tungsten tiles are to be used elsewhere on the divertor (see areas marked Be, C and W in Fig. 1). Tungsten is very resistant to high temperatures (melting only at 3695 degrees Celsius) but it is a heavy element (proton number 74) that can pollute plasmas considerably: it gets highly ionised in extreme plasma temperatures which causes immense energy losses due to plasma radiation, and dilutes the D-T fuel. Beryllium is a light element with a proton number just 4. However it melts at just 1284 degree Celsius. The combination of beryllium and tungsten has never been tested in a tokamak, let alone in one with ITER-relevant geometry and plasma parameters like JET.

During the one year installation period in 2008, extensive use of Remote Handling technology will be made in implementing the beryllium first wall and tungsten divertor. Following installation, the JET experimental programme will focus on optimising operating scenarios compatible with the ITER-like wall. The level of retained tritium and its dependence on plasma parameters will be determined. Plasma performance will be tested to show that the level of tungsten reaching the core is acceptably low. The lifetime of the wall will be studied with ITER-relevant power loading provided by increased heating due to Neutral Beam Enhancement Project. Also notice the synergy in the pan-European fusion research: while ASDEX Upgrade tokamak (Association Euratom-IPP Garching, Germany) is exploring the viability of an all-Tungsten first wall (tungsten is considered the long-term front runner as a material for fusion reactors), JET will be looking at more immediate ITER needs.

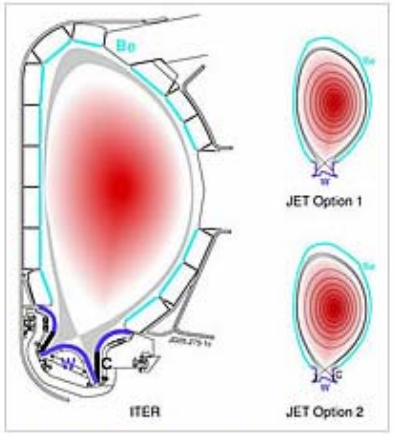

Fig. 1 ITER wall and two options for JET's ITER-like Wall Project (to scale)

http://www.jet.efda.org/pages/jet-iter/wall/index.html

Carbon – Tungsten

merit

low radiation at core

demerit

high erosion

tritium co-deposition

damaged by neutrons

merit

low erosion

no tritium co-deposition

resistant to neutrons

demerit

high radiation cooling at core

Tungsten concentration

1977

Electron temperature profile in PLT
Tungsten accumulation

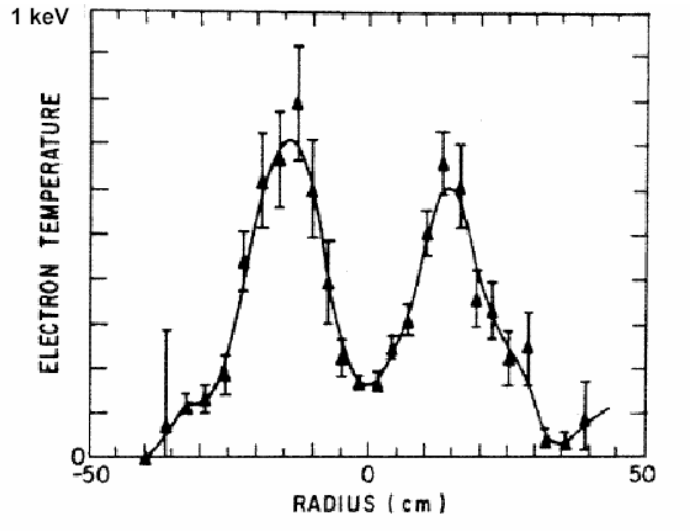

Wall conditioning by boronization
sufficient additional heating power

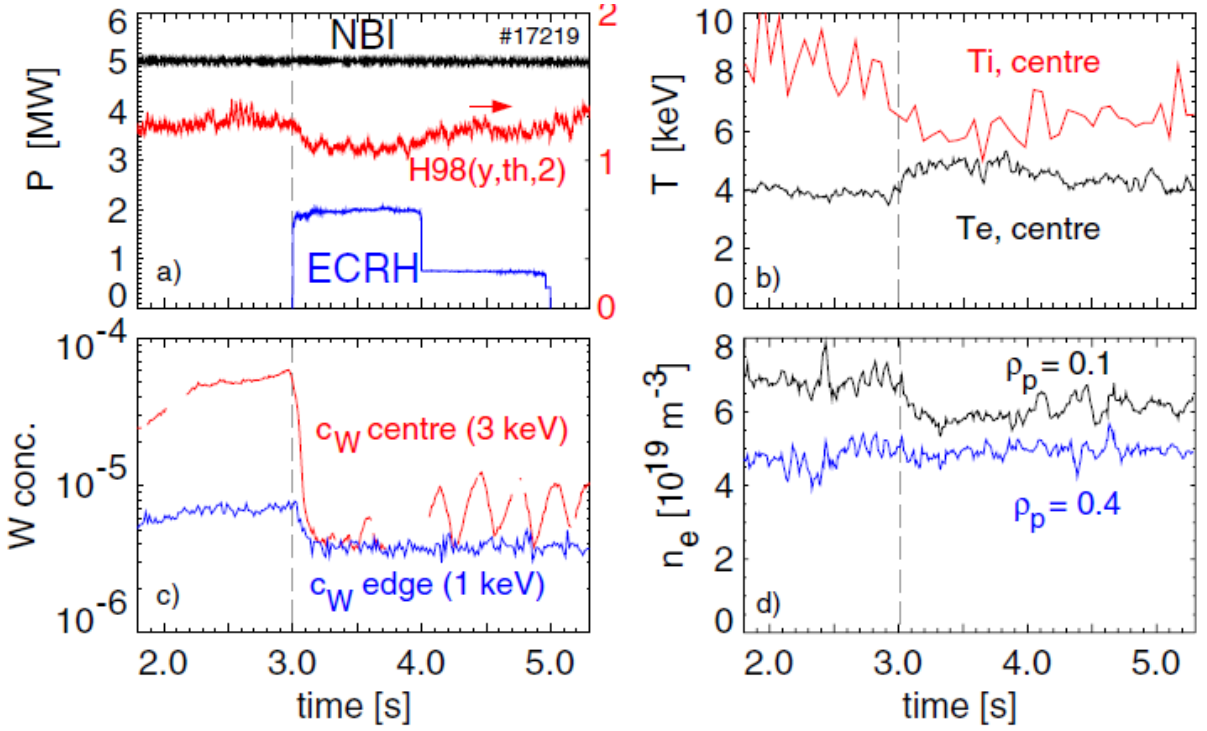

Application of central ECRH
cure the central tungsten concentration

(tungsten PFC)

ASDEX Upgrade

A. Kallenbach et al. PPCF 47 (2005) B207

Spectrum from W I in tokamaks

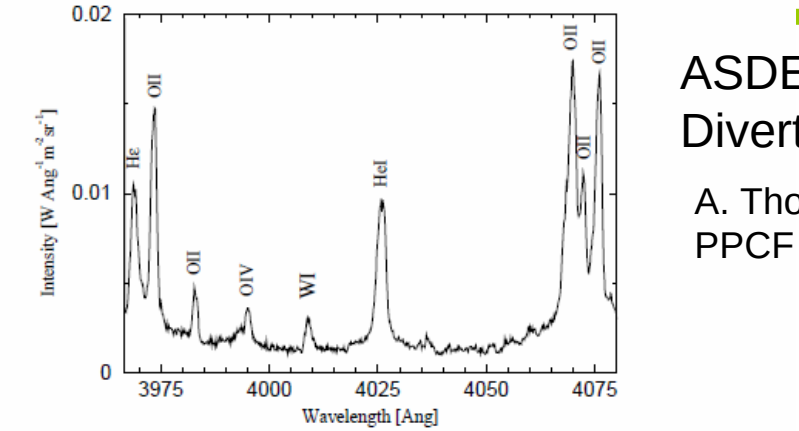

ASDEX Upgrade
Divertor strike point

A. Thoma, K. Asmussen, R Dux, et al.
PPCF **39** (1997) 1487

Figure 2. Typical spectrum near the WI emission line. This spectrum was recorded at the strike point with 9 ms exposure time in a 1 MA ohmic discharge with a line-averaged electron density of 3×10^{19} m^{-3} in the main plasma. The spectrometer allows the simultaneous observation of several emission lines of oxygen, helium and hydrogen that are close to the prominent WI emission at 400.9 nm.

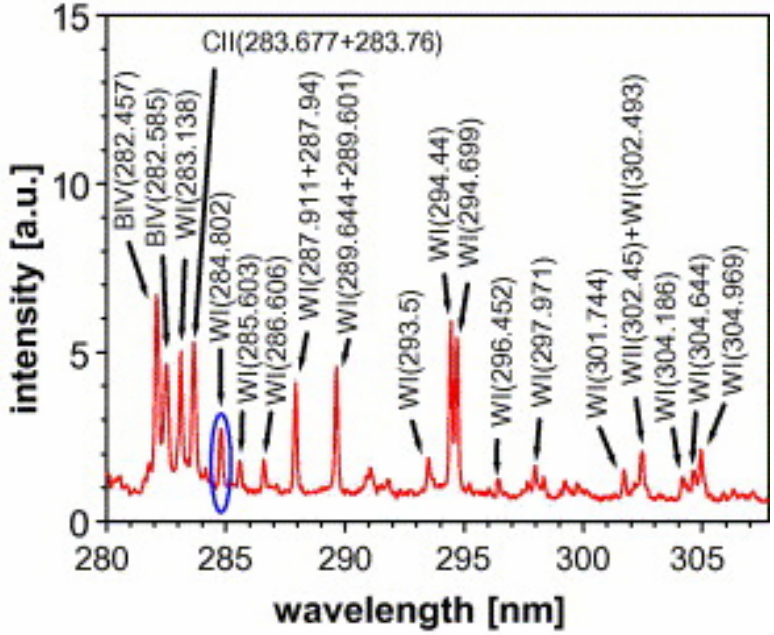

Sergienko, et al., J of Nucl. Mater.
363-365, (2007), 96-100

limiter in TEXTOR

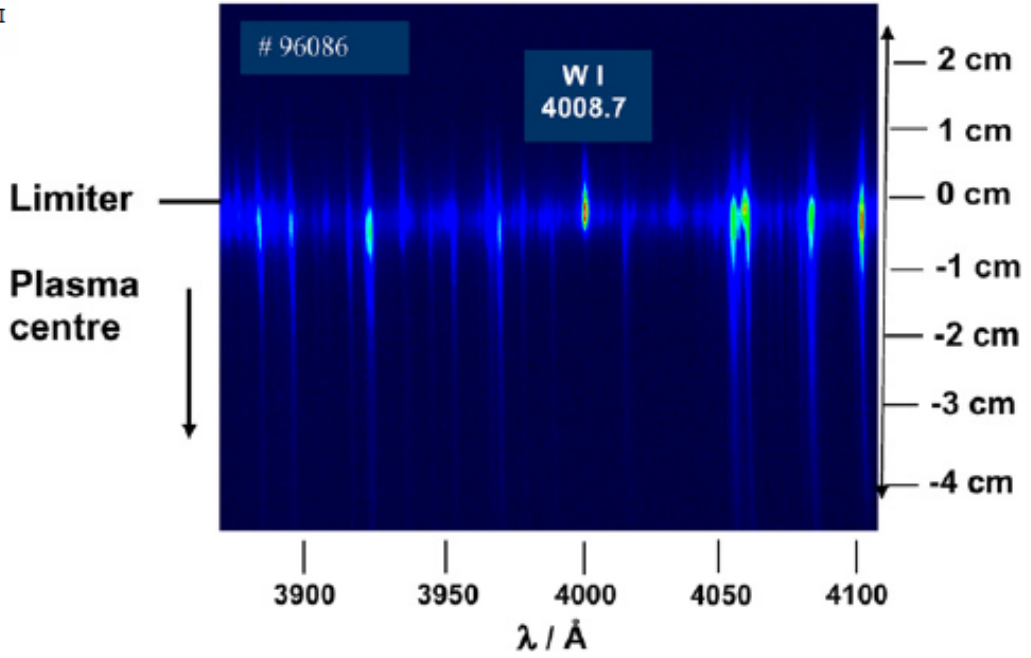

I. Beigman, A. Pospieszezyk, G. Sergienko et al.
PPCF49 (2007) 1833

influx determination from integral line intensity

The flux $\Phi(r)$ of atoms with velocity of v_A is assumed be equivalent to the number of ionization events:

$$\Phi_A = \int_{r_1}^{r_2} n_A(r) n_e(r) \langle \sigma_I v_e \rangle \mathrm{d}r$$

$$\Phi_A = 4\pi \frac{I_{tot}}{h\nu} \frac{S}{XB}$$

$$S \equiv \langle \sigma_I v_e \rangle$$

$$X \equiv \langle \sigma_{Exg} v_e \rangle$$

$$B \equiv \Gamma$$

ASDEX Upgrade
For tungsten (S/XB) = 20 was used

R. Dux, et al. JNM 337-339 (2005) 852

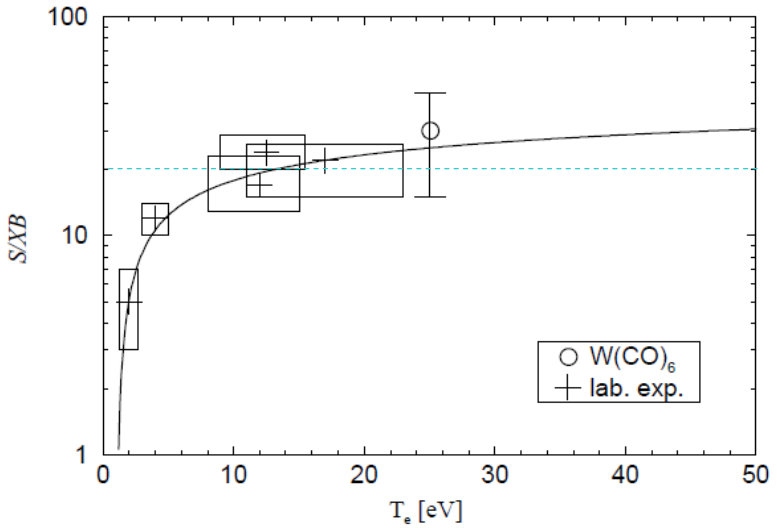

Figure 3. Temperature dependence of S/XB for the WI emission line at 400.9 nm. The values below 20 eV are deduced from a laboratory experiment [12]. The boxes indicate the error bars for the marked S/XB values (+). For higher electron temperatures $W(CO)_6$ was sublimed from an oven mounted in the ASDEX Upgrade divertor. The intensity ratio of the WI to the OII emission is used to derive S/XB (○) [15].

A. Thoma, et al. PPCF 39 (1997) 1487

A.Pospieszczk Diagnostics of Edge Plasmas by Optical Methods
R.K. Janev and H.W. Drawin eds. Atomic and Plasma-Material Interaction processes in controlled thermonuclear fusion, Elsevier 1993, p213

Grotrian Diagram of W I

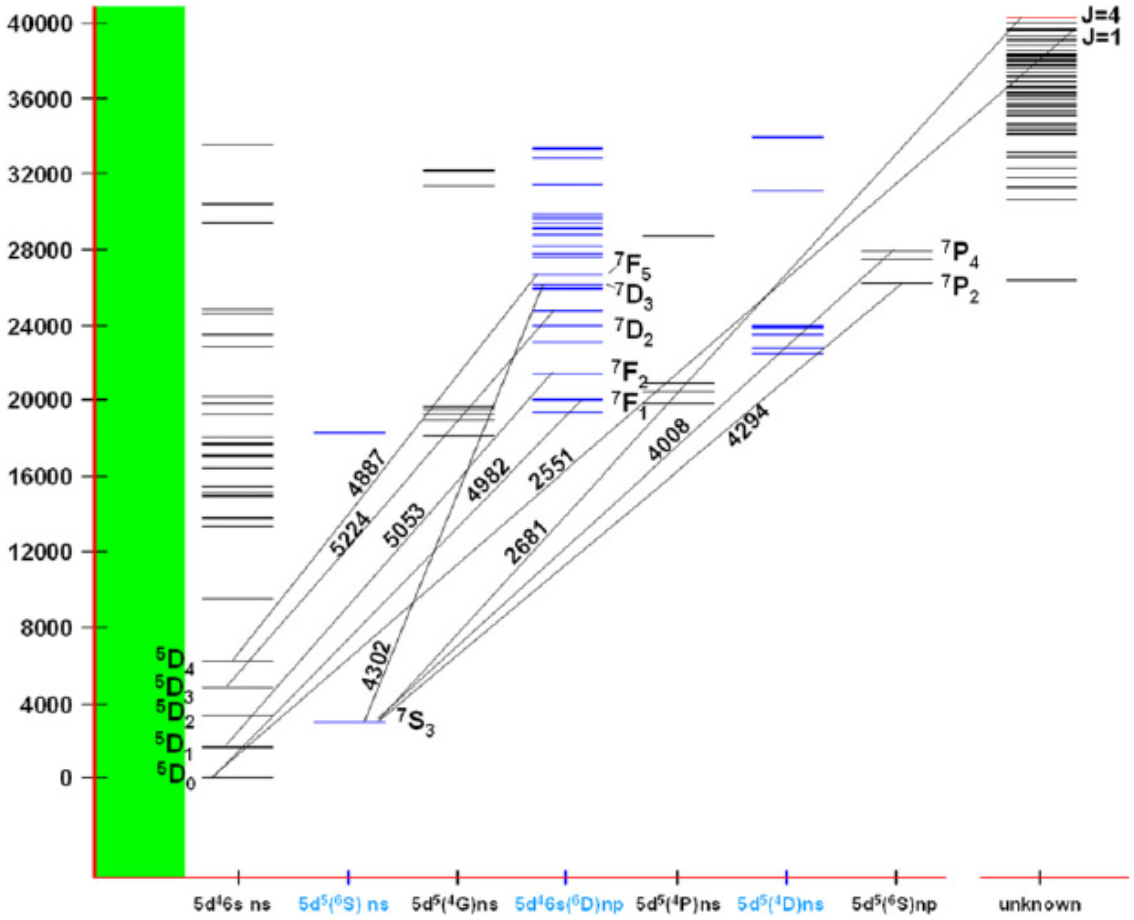

Figure 2. Reduced Grotrian diagram of W I (from [10]).

I. Beigman, A. Pospieszezyk, G. Sergienko et al.
PPCF49 (2007) 1833

coronal approximation from ground levels

Dipole transition

Excitation: semi-empirical van Renenmorter formula

$$\langle v\sigma_{k_0,k}\rangle = 0.11\times 10^{-16}\cdot\frac{g_k}{g_{k_0}}A_{k,k_0}\left(\frac{Ry}{\Delta E}\right)^3 u(T_e)e^{-\beta_{ex}}\ (\mathrm{cm^3\ s^{-1}}),$$

$$u(T_e)=\beta^{0.5}\log(2+1/(1.78\beta_{ex})),\qquad \beta_{ex}=\Delta E/T_e,\quad \beta=Ry/T_e,$$

Ionization: Born-Ochkur approximation

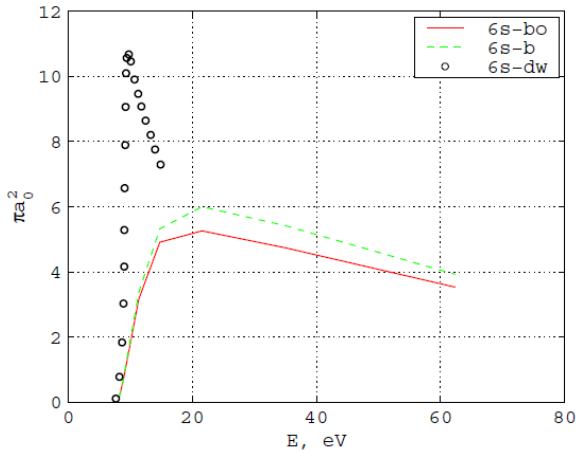

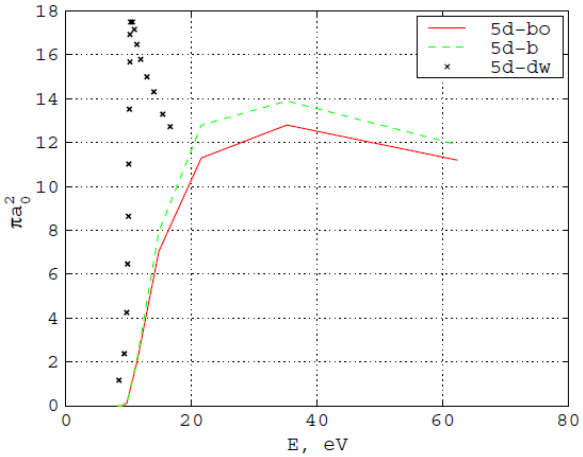

I. Beigman, A. Pospieszezyk, G. Sergienko et al.
PPCF49 (2007) 1833

S/XB for W I 400.8 nm

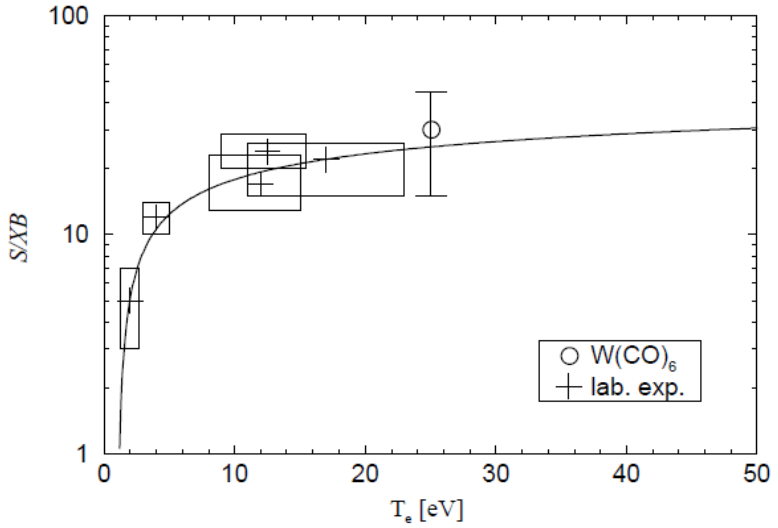

Figure 3. Temperature dependence of S/XB for the WI emission line at 400.9 nm. The values below 20 eV are deduced from a laboratory experiment [12]. The boxes indicate the error bars for the marked S/XB values (+). For higher electron temperatures $W(CO)_6$ was sublimed from an oven mounted in the ASDEX Upgrade divertor. The intensity ratio of the WI to the OII emission is used to derive S/XB (○) [15].

T_w: ground level population distribution

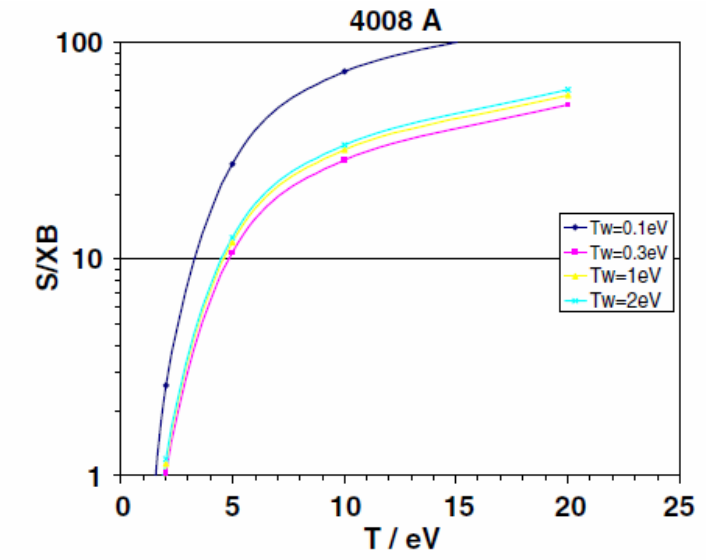

I. Beigman, A. Pospieszezyk, G. Sergienko et al. PPCF49 (2007) 1833

Specification for plasma measurements on ITER - impurity influx monitor (divertor) -

Measurement	Parameter	Condition	Range or Coverage	Resolution: Time or Freq.	Resolution: Spatial or Wave No.	Accuracy
12. Impurity species monitoring	Be, C rel. conc.		10^{-4}–5×10^{-2}	10 ms	Integral	10% (rel.)
	Be, C influx		4×10^{16}–2×10^{19} s^{-1}	10 ms	Integral	10% (rel.)
	Cu rel. conc.		10^{-5}–5×10^{-3}	10 ms	Integral	10% (rel.)
	Cu influx		4×10^{15}–2×10^{18} s^{-1}	10 ms	Integral	10% (rel.)
	W rel. conc.		10^{-6}–5×10^{-4}	10 ms	Integral	10% (rel.)
	W influx		4×10^{14}–2×10^{17} s^{-1}	10 ms	Integral	10% (rel.)
	Extrinsic (Ne,Ar, Kr) rel. Conc.		10^{-4}–2×10^{-2}	10 ms	Integral	10% (rel.)
	Extrinsic (Ne, Ar, Kr)		4×10^{16}–8×10^{18} s^{-1}	10 ms	Integral	10% (rel.)
35. Impurity and D,T influx in the divertor	Γ_{Be}, Γ_C, Γ_W		10^{17}–10^{22} at s^{-1}	1 ms	50 mm	30%
	Γ_D, Γ_T		10^{19}–10^{25} at s^{-1}	1 ms	50 mm	30%
39. Divertor helium density	n_{He}		10^{17}–10^{21} m^{-3}	1 ms	—	20%
40. Fuel ratio in the divertor	n_T/n_D		0.1–10	100 ms	integral	20%
	n_H/n_D		0.01–0.1	100 ms	integral	20%

Progress in the ITER Physics Basis

A.J.H Donné, A.E. Costley, R. Barnsley et al. Nuclear Fusion 47 (2007) S337-S384

D, T atoms and molecules

- Edge Plasma Modeling
  - Monte-Carlo simulation
    - Neutral-neutral collision
    - Radiation transport

      (in *B* field: Zeeman component Polarization?)
  - Molecules
    - Vibrational excitation of D_2, (DT, T_2 ?)
    - Rotational excitation

D, T atoms and molecules

- Edge Plasma Modeling
  - Monte-Carlo simulation
    - Geometry
    - Neutral-neutral collision
    - Radiation transport

      (in *B* field: Zeeman component Polarization?)
  - Molecules
    - Vibrational excitation of D_2, (DT, T_2 ?)
    - Rotational excitation